Viscous fingering of miscible fluids in an anisotropic radial Hele-Shaw cell: Coexistence of kinetic and surface-tension dendrite morphology types and an exploration of small-scale influences

A. G. Banpurkar, Abhijit S. Ogale, and A. V. Limaye
Department of Physics, University of Pune, Pune 411 007, India

S. B. Ogale
Department of Physics, University of Maryland, College Park, Maryland 20742

(Received 22 January 1998; revised manuscript received 12 October 1998)

The evolution of viscous fingering morphology is examined for the case of a system of miscible fluids in an anisotropic radial Hele-Shaw cell. It is shown that dendritic morphologies similar to the kinetic and surface-tension morphology types coexist for this case. The critical role of the means of introducing anisotropy in the Hele-Shaw cell is established, and an explanation of the pattern behavior is offered on the basis of shape discontinuities of the individual elements of the lattice used to induce anisotropy. The ramifications of such an explanation are experimentally verified by demonstrating a clear difference in the morphology evolution in two halves of a single Hele-Shaw cell, one half of which contains square lattice elements, and the other half of which contains circular lattice elements. [S1063-651X(99)14202-8]

PACS number(s): 68.70.+w, 47.20.Ma, 47.54.+r, 68.10.−m

In the case of widely studied diffusion controlled systems, and in the presence of anisotropy, it has been possible to identify a set of essential morphology types [1–5] which evolve depending upon the degree of departure from equilibrium and the nature of interfacial dynamics. In a random growth environment, the development of patterns having different morphologies poses questions relating to the existence of a possible selection mechanism [4,5]. Another issue which arises in this context is the following: why is it that morphology types are hardly seen to coexist? Ben-Jacob *et al.* [6] analyzed this issue in some detail.

Experiments on fluid flow in an anisotropic radial Hele-Shaw cell and on two-dimensional electrodeposition have brought out several specific morphology types such as faceted, tip splitting, and dendrite morphologies [5–7]. Subsequently, Ben-Jacob *et al.* [8] presented experimental evidence for an additional distinct morphology type, namely, dense branching morphology, as a fundamental pattern in diffusion controlled growth. In yet another study, Ben-Jacob *et al.* (Ref. [10]; also see Ref. [9]) examined the nature of the morphology transition in diffusion controlled systems, and highlighted the importance of the interplay of surface tension and kinetic effects in the selection of the morphology type. The experiments performed thus far on miscible liquid displacements have been relatively few in number, as pointed out by Lajeunesse *et al.* [11], and are restricted to the case of an isotropic Hele-Shaw cell [12–14]. The issue of miscible viscous fingering in a percolation medium has been addressed [15,16], and these studies have highlighted the importance of several parameters such as the mobility ratio, dispersion, gravity, and heterogeneity of the porous medium.

In order to gain further insights into the issue of morphology selectivity, we decided to undertake a study of pattern formation in the process of viscous fingering in an anisotropic radial Hele-Shaw cell using a system of miscible liquids. As shown in this work, the loss of a well defined (sharp) interface caused by a marginal mixing of the fluids has remarkable consequences for the viscous fingering process; the corresponding patterns show, for the first time, the coexistence of surface-tension and kinetic dendrite morphology types. The origin of the observed differences in the behavior of the miscible and immiscible fluids can be traced to the small-scale influences of the surface curvature discontinuities of the grids used to introduce the anisotropy. Justification for this explanation is provided by demonstrating a clear difference in the morphology evolution in two half planes of square and circular grids in a single Hele-Shaw cell.

The experimental anisotropic radial Hele-Shaw cell used by us is comprised of two 1-cm-thick, $30\times30\text{-cm}^2$ float-glass plates. Anisotropy was introduced using a patterned copper circuit board, which was placed on the bottom supporting glass plate. A square lattice of square-shaped lattice elements (henceforth referred to as ''grid cells'') was etched onto the circuit board. The dimension of each copper grid cell was $0.85\times0.85\,\text{mm}^2$, the intergrid cell separation was 0.70 mm, and the height of the grid cell was 70 μm. High viscosity glycerine (the viscosity is 850 cP and the surface tension is 63 dyne/cm) and water dyed with ink (the viscosity is 1.1 cP and the surface tension is 72 dyne/cm) were used as the displaced and displacing fluids respectively. The displacing liquid was injected through a hole drilled at the center of the top plate using an automated fluid delivery system. The experiments were performed with the plate separation (including height of grid cell) ranging from 70 μm (touching) to 400 μm, and the volume flow rate ranging from 0.2 to 30 ml/min.

Within the anisotropy dominated regime, it is observed that, for the miscible fluid system, the viscous fingering dendrites grow simultaneously along the directions of the channels (kinetic dendrites) as well as along the directions, making an angle of 45° with the channel directions (similar to

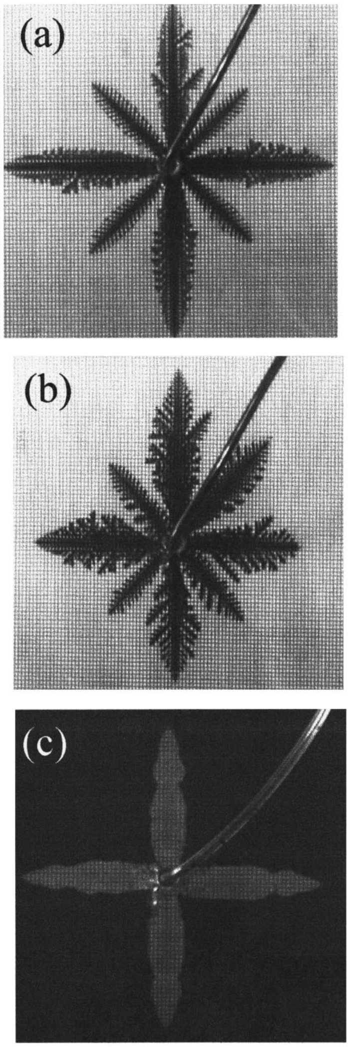

FIG. 1. Dendrite morphology in the case of miscible water glycerine system with volume flow rates (VFR's) of (a) 0.18 ml/min and (b) 30 ml/min. (c) Immiscible kerosene glycerine system with a VFR of 0.4 ml/min. (The plate separation is at 270 μm for all cases.)

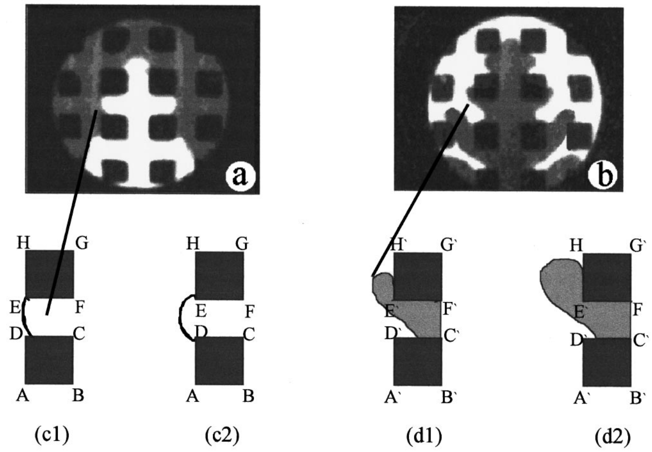

FIG. 2. Zoomed images for (a) the immiscible kerosene-glycerine system [schematics (c1) and (c2)], and (b) miscible water-glycerine system [schematics (d1) and (d2)].

surface tension dendrites), in remarkable contrast to the case of immiscible fluids which exhibit one or the other morphology type [9,10] in this situation. This is shown in Figs. 1(a) and 1(b), wherein the fingering morphology patterns for the miscible glycerine-water system are presented for two very different volume flow rates. To our knowledge, this is the first demonstration of the coexistence of kinetic and surface-tension dendrite morphology types in any two fluid system in an anisotropic radial Hele-Shaw cell. It may be pointed out that the side branching scheme for the case of miscible fluids is also distinctly different as compared to the immiscible fluid system. For instance, the side branches on the primary kinetic dendrites grow at 45° for the case of miscible fluids, and at 90° for the case of immiscible fluids [5]. The additional significant feature of the result in the case of a miscible system is its insensitivity to the wide variation in the flow rates. A similar growth of the coexisting kinetic and surface-tension dendrite morphology types was also verified using another miscible fluid system: the oil-kerosene system.

The morphology selection in the case of immiscible systems has been well studied by many researchers [5,6,9,10,17]. As stated earlier, in such systems, simultaneous growth of kinetic and surface-tension dendrites does not occur. We also performed experiments for immiscible systems on our own experimental setup. Figure 1(c) shows the morphology for the immiscible glycerine-kerosene liquid system for a volume flow rate of 0.4 ml/min, and for a plate separation of 270 μm. The absence of the coexistence of surface-tension and kinetic dendrites can be clearly noted in this case.

Dendritic morphology for the miscible fluid system was also analyzed in terms of the self-similar scaling behavior [18] $x \sim t^{\alpha}$ and $y \sim t^{1-\alpha}$, where x is the longitudinal coordinate and y the transverse coordinate of each of the primary fingers. Such characterizations have been analytically derived [18] and also experimentally verified [17] for systems of immiscible fluids. We studied the dependence of the scaling behavior of x and y on time for various flow rates. Fingertip positions of both kinetic and surface-tension types of dendrites were seen to follow the power law $x_{\text{tip}} \propto t^{\alpha}$, where the power law exponent yields $\alpha = 0.56 \pm 0.04$ for the kinetic dendrite and $\alpha = 0.58 \pm 0.06$ for the surface-tension type dendrite. It is remarkable that the coexisting kinetic and surface-tension types of dendrites in the miscible case yield values of the power law exponent α which match with the values obtained for the corresponding independently developing dendrites in the immiscible case within the error limits [17].

In order to elucidate the cause of the dramatic difference in the pattern features observed for the cases of the immiscible and miscible fluids, we analyzed the zoomed image of a very small region comprised of a few grid cells, and examined the local flow patterns. Two such patterns for the immiscible and miscible cases are shown in Figs. 2(a) and 2(b) respectively. For the immiscible case, no growth along the edge *EH* [Figs. 2(a) and 2(c1)] takes place until such time as the capillary space *DCFE* between the two grid cells is filled by the displacing fluid. This behavior is indeed expected, since the finger growth in the immiscible case evolves solely as a consequence of the surface tension and driving force systems. The curvature discontinuity at point *E* pins the fluid-fluid interface, thereby arresting its propagation along edge *EH*. For the miscible case, however [Figs. 2(b) and 2(d1)], the extra element of mixing of the fluids results in the

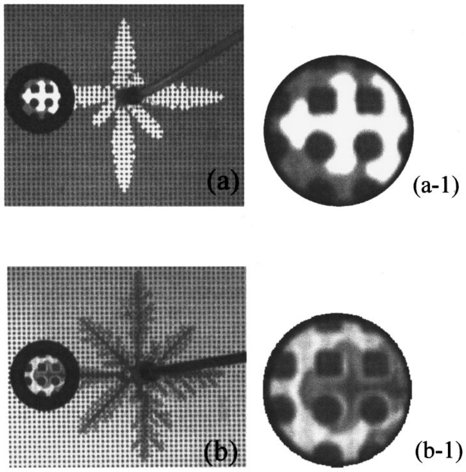

FIG. 3. Copper grid cells are square shaped in the upper half plane of the circuit board and are circular shaped in the lower half plane. (a) The immiscible kerosene glycerine system produces extra diagonal branches in the lower half plane. (The VFR is 0.06 ml/min.) (a-1) Zoomed image of the encircled region in (a). (b) The miscible water glycerine system shows no influence of the difference in grid cell shape in the two half planes. (The VFR is 0.06 ml/min.) (b-1) Zoomed image of the encircled region in (b). The plate separation is 70 μm (plates are touching) for both cases.

loss of a sharp interface near point E', thereby eliminating the issue of pinning at point E' altogether. This results in the propagation of the diffused interface beyond point E' much before the capillary space $D'C'F'E'$ between the two grid cells fills up. Once the diffused interface passes along to the edge $E'H'$, growth along that edge has a considerably higher preference than growth along the edge $C'D'$. This is because the fluid flowing along the $C'E'$ curve has a net radially outward pressure gradient pushing the displacing liquid toward E', and then along the edge $E'H'$. Thus, in the miscible case, surmounting of the curvature discontinuity at point E' escalates growth along the edge $E'H'$ [Figs. 2(b) and 2(d2)]. As a result, the portion $D'C'F'E'$ between the two grid cells is left partially filled. This should lead to the development of 45° side branches only in the miscible case, as is indeed experimentally observed. Here we see the importance of the miscibility effects at points identical to point E', and perceive their effect on the geometry of the entire pattern. This is a classic example in which the critical conditions at a single point affect the entire pattern geometry.

It should be emphasized that even a very small amount of mixing at point E' will cause the interface to become sufficiently diffused so as to overcome the curvature discontinuity at such points, and enable the diffused interface to propagate beyond that point prior to the filling up of the region between the grid cells. It can easily be judged that the time required for the microscopic mixing, which is sufficient to overcome the curvature discontinuity, is very much smaller than the time required for the capillary space $D'C'F'E'$ to fill up completely. This should explain the invariance of the gross features of the branching scheme in miscible systems, although parameters such as flow rate, surface tension, etc. were significantly varied. The above explanation for 45° side branching along one branch applies equally well to the growth of the 45° primary branches at the fluid injection center in the miscible case.

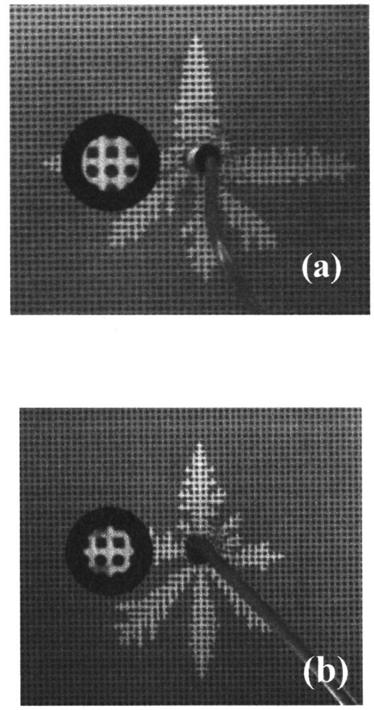

FIG. 4. Copper grid cells are square shaped in the upper half plane of the circuit board, and circular shaped in the lower half plane. (a) Immiscible kerosene-glycerine system: The volume flow rate is 0.06 ml/min, and the plate separation is 100 μm (plates are not touching). (b) Immiscible kerosene-glycerine system: The volume flow rate is 0.14 ml/min, and the plate separation is 70 μm (plates are touching)

As pointed out above, the case studied in the present work corresponds to a situation wherein the width of the transition zone between the two fluids is much smaller than the confining channel widths over the time scale of pattern development. There could be situations wherein the width of the transition zone between the fluids is comparable to the other length scales involved in the problem. The details regarding morphology evolution in such cases will have to be explored separately.

One would expect from the above discussion that, if circular grid cells rather than square ones are used, one should obtain 45° primary branches even for the immiscible system as for the miscible system of fluids. To verify this experimentally, a copper circuit board with square grid cells in one half plane, and circular grid cells in the other half plane, was used in the radial Hele-Shaw cell setup. The fluid injection point was in the middle of the Hele-Shaw cell on the boundary between the regions containing circular and square grid cells. This arrangement was used to avoid the errors arising from small differences in the experimental conditions, which could come about if separate experiments were conducted using square and circular grid cells. The square and circular grid cells were chosen to have the same area. In these experiments, plate separation was kept at 70 μm (i.e., plates were touching). The immiscible kerosene glycerine system at volume flow rate of 0.06 ml/min produced the pattern shown in Fig. 3(a). In the figure, the lower half plane contains circulargrid cells, and the upper half plane contains square grid cells. (This is immediately evident from the adjoining zoomed images.) It can be clearly seen that the primary diagonal (45°) branches appear only in the lower half plane containing the circular grid cells. Figure 3(a-1) highlights the small scale aspects of the growth of the interface. Since all the other influencing parameters are identical in the two half planes, one is consigned to conclude that the drastic differences in the patterns in the two halves are a direct consequence of the difference in the shape of the grid cells. To verify this aspect even further, we conducted an experiment using the above assembly and under the same experimental conditions, employing the miscible liquid water-glycerine system. This system produces the pattern shown in Fig. 3(b). It is clearly seen that the pattern formation in this case does not make much distinction between the region containing circular grid cells and the region containing square grid cells. Figure 3(b-1) highlights the small scale aspects of the propagation of the diffused interface. This experiment further strengthens our explanation, which stresses the inability to pin a diffused fluid-fluid interface at the grid discontinuities, as a consequence of the fluid miscibility.

In the case of the immiscible kerosene-glycerine system, experiments were also performed at different (but small) plate separations and various flow rates. The pattern obtained by changing the plate separation for the immiscible kerosene-glycerine system is shown in Fig. 4(a), and we again observe the 45° diagonal branches only in the lower half plane, which contains circular grid cells. The flow rate was the same as for the case of Fig. 3(a). As the flow rate was increased, small stubs were seen to grow in the diagonal (45°) directions even in the half plane containing the square grid cells [Fig. 4(b)]. Such stubs were much smaller than their counterparts in the half plane containing the circular grid cells. In the context of our proposed explanation, this aspect may be viewed as follows: At a higher flow rate, the interface propagation in the immiscible case may have a large enough kinetic contribution to overcome the pinning at the edge discontinuities. Thus, at a high enough flow rate, even the immiscible fluid system will begin to show the 45° primary diagonal branches even in the region containing square grid cells.

We further wish to emphasize that all the previous work on viscous fingering in an anisotropic radial Hele-Shaw cell primarily focused on the global aspects of anisotropy and their implications for morphology selection. Our work demonstrates that local geometric features are equally important in this context in view of the intrinsically sequential nature of pattern evolution in such systems. We believe that our findings will be of significant interest in the context of a broad class of problems involving fluid flows in confined systems and porous media, and related situations in physical, chemical, and biological systems.

In summary, we have examined the evolution of viscous fingering morphology for the case of a system of miscible fluids in an anisotropic radial Hele-Shaw cell. It is shown that the kinetic and surface tension dendrite morphology types coexist for this case irrespective of the strength of the driving force. This occurrence is attributed to the miscibility induced modifications of the critical interface propagation conditions at the edge discontinuities of the grid cells. The effects of the above hypothesis are verified by removing the edge discontinuities of the grid cells (by using circular shaped grid cells), and observing the growth of the surface-tension type dendrites even in the case of the immiscible liquid system.

Two of the authors (A.G.B. and A.V.L.) acknowledge financial support from CSIR and DST (Government of India), respectively.

[1] J. S. Langer, Rev. Mod. Phys. **52**, 1 (1980).
[2] E. Ben-Jacob, O. Schochet, A. Tenenbaum, I. Cohen, A. Czirok, and T. Vicsek, Nature (London) **368**, 46 (1994).
[3] *Fractal Growth Phenomena*, edited by T. Vicsek (World Scientific, New York, 1992).
[4] L. Zeiri, O. Younes, S. Efrima, and M. Deutsch, Phys. Rev. Lett. **79**, 4685 (1997).
[5] E. Ben-Jacob and P. Garik, Nature (London) **343**, 523 (1990).
[6] E. Ben-Jacob, R. Godbey, N. D. Goldenfeld, J. Koplik, H. Levine, T. Mueller, and L. M. Sander, Phys. Rev. Lett. **55**, 1315 (1985).
[7] D. Grier, E. Ben-Jacob, R. Clarke, and L. M. Sander, Phys. Rev. Lett. **56**, 1264 (1986).
[8] E. Ben-Jacob, G. Deutscher, P. Garik, N. D. Goldenfeld, and Y. Lareah, Phys. Rev. Lett. **57**, 1903 (1986).
[9] V. Horvath, T. Vicsek, and J. Kertesz, Phys. Rev. A **35**, 2353 (1987).
[10] E. Ben-Jacob, P. Garik, T. Mueller, and D. Grier, Phys. Rev. A **38**, 1370 (1988).
[11] E. Lajeunesse, J. Martin, N. Rakotomalala, and D. Salin, Phys. Rev. Lett. **79**, 5254 (1997).
[12] R. A. Wooding, J. Fluid Mech. **39**, 477 (1969).
[13] L. Paterson, Phys. Fluids **28**, 26 (1985).
[14] G. Daccord, J. Nittmann, and H. E. Stanley, Phys. Rev. Lett. **56**, 336 (1986).
[15] G. M. Homsy, Annu. Rev. Fluid Mech. **19**, 271 (1987); D. E. Moissis, C. A. Miller, and M. F. Wheeler, in *Numerical Simulation in Oil Recovery* edited by M. F. Wheeler (Springer-Verlag, New York, 1988), Vol. 11, p. 227.
[16] M. Sahimi and A. O. Imdakm, J. Phys. A **21**, 3833 (1988).
[17] J. Ignes-Mullol and J. V. Maher, Phys. Rev. E **53**, 3788 (1996).
[18] R. Almgren, Wei-Shen Dai, and V. Hakim, Phys. Rev. Lett. **71**, 3461 (1993).